Nanoscale

PAPER

View Article Online
View Journal | View Issue

Cite this: *Nanoscale*, 2014, **6**, 2887

Fullerene-driven encapsulation of a luminescent Eu(III) complex in carbon nanotubes†

Laura Maggini,[ab] Melinda-Emese Füstös,[cd] Thomas W. Chamberlain,[e] Cristina Cebrián,[b] Mirco Natali,[bf] Marek Pietraszkiewicz,[g] Oksana Pietraszkiewicz,[g] Edit Székely,[h] Katalin Kamarás,[c] Luisa De Cola,[b] Andrei N. Khlobystov[e] and Davide Bonifazi*[ai]

Received 4th November 2013
Accepted 5th December 2013

DOI: 10.1039/c3nr05876j

www.rsc.org/nanoscale

A novel CNT-based hybrid luminescent material was obtained *via* encapsulation of a C_{60}-based Eu(III) complex into single-, double- and multi-walled carbon nanotubes (SWCNTs, DWCNTs and MWCNTs, respectively). Specifically, a luminescent negatively charged Eu(III) complex, electrostatically bonded to an imidazolium-functionalized fullerene cage, was transported inside CNTs by exploiting the affinity of fullerenes for the inner surface of these carbonaceous containers. The filling was performed under supercritical CO_2 ($scCO_2$) conditions to facilitate the entrapment of the ion-paired assembly. Accurate elemental, spectroscopic and morphological characterization not only demonstrated the efficiency of the filling strategy, but also the occurrence of nano-ordering of the encapsulated supramolecular luminophores when SWCNTs were employed.

Introduction

Along with an increase of the available methodologies for their manipulation,[1] and the development of atomic-resolution visualization techniques, mainly high-resolution transmission electron microscopy (HRTEM),[2] carbon nanotubes (CNTs)[3] are increasingly attracting attention towards the study and exploitation of their porous properties. Indeed, CNTs can be employed as nano-containers, nano-reactors, or as fillable conductive nano-vessels, able to give rise to advanced hybrid graphitic materials utilizable in both electronic and nano-biotechnological devices.[4]

The feasibility of the entrance of guest molecules within the inner channel of CNTs relies on the favorable establishment of a range of interactions between the "guest" molecules and the "host" CNTs,[5] amongst which van der Waals forces often appear to be predominant.[6] These are maximized when the host–guest complex occurs between CNTs and related graphitic materials,[7] such as fullerenes, *e.g.* C_{60} and C_{70}. In fact, the common nature of the two materials, together with the perfect geometrical match of the shape of a fullerene and the inner nanotube surface of single-walled CNTs (SWCNTs), results in a spontaneous encapsulation.[8]

The use of CNTs as templating nano-containers has recently started to draw attention as a possible strategy for the synthesis of novel highly organized photonic materials. It is well established that the emission properties of a chromophore, in terms of color and intensity, are extremely sensitive to the environment.[9–11] Encapsulation of luminophores within a protective "cage" (*i.e.* CNTs) might hence grant a sheltering effect from hostile reactive species, as demonstrated by Yanagi *et al.* with the long-lasting luminescence of β-carotene encapsulated in SWCNTs.[12] Furthermore, molecular confinement in such a restrained space might induce an ordered mono-dimensional molecular arrangement, potentially characterized by unique architecture-dependent emission properties. At present only a relatively limited number of luminescent guests have been successfully inserted inside CNTs and their emissive properties investigated.[13] Among these, a prime example of the templating action of CNTs on internalized luminescent molecules has been described for the encapsulation of coronenes in SWCNTs.[14,15]

[a]*Namur Research College (NARC), and Department of Chemistry, University of Namur (UNamur), Rue de Bruxelles 61, 5000 Namur, Belgium. E-mail: davide.bonifazi@unamur.be*

[b]*Institut de Science et d'Ingénierie Supramoléculaires (ISIS), Alleé Gaspard Monge 8, 67000 Strasbourg, France*

[c]*Institute for Solid State Physics and Optics, Wigner Research Centre for Physics, Hungarian Academy of Sciences, Konkoly-Thege M. 29-33, 1121 Budapest, Hungary*

[d]*Faculty of Chemistry and Chemical Engineering, Babeș-Bolyai University, Arany János 11, 400028 Cluj-Napoca, Romania*

[e]*School of Chemistry, University of Nottingham, University Park, Nottingham NG7 2RD, UK*

[f]*Department of Chemical and Pharmaceutical Sciences, University of Ferrara, Via Fossato di Mortara 17-19, 44121, Ferrara, Italy*

[g]*Institute of Physical Chemistry, Polish Academy of Sciences, PL-01224 WarsawKasprzaka 44/52, Poland*

[h]*Department of Chemical and Environmental Process Engineering, Budapest University of Technology and Economics, Budafoki út 8, 1111 Budapest, Hungary*

[i]*Department of Chemistry and Pharmaceutical Sciences, INSTM UdR Trieste, University of Trieste (UNITS), Piazzale Europa 1, 34127 Trieste, Italy*

† Electronic supplementary information (ESI) available: Experimental details, XPS, TGA, ATR-IR, PL analysis, and additional HRTEM images. See DOI: 10.1039/c3nr05876j

Lanthanide β-diketonate complexes (LnCs)[16] are among the most investigated rare earth coordination compounds. Regrettably, despite their exceptional luminescent properties, their low thermal and photochemical stability,[17] together with their tendency to aggregate or coordinate solvent water molecules undergoing quenching inter-chromophoric interactions, often limit their utilization. Attempts to enhance the mechanical properties of LnCs have been accomplished taking advantage of several scaffolding materials.[16,18,19] In a seminal collaborative report, we described a simple and straightforward methodology to prepare LnC–CNT hybrids by direct adsorption of a neutral Eu(III)-based LnC onto oxidized single-walled CNTs (ox-SWCNTs) *via* hydrophobic interactions, obtaining a strongly emitting composite in which the structural and electronic properties of both constituents remained preserved.[20] Since then, different approaches to blend CNTs and LnCs have been reported.[21–24] Among these, our group specifically developed new exohedral supramolecular functionalization methodologies with Eu(III)-based complexes.[25–27] In particular, by means of electrostatic interactions, negatively charged Eu(III) complexes were used to positively decorate charged multi-walled CNTs (MWCNTs) forming stable and luminescent hierarchized architectures.[25–27]

Intrigued by the possibility of exploring the effect of encapsulation on the luminescent output of LnCs, we have recently tackled the filling of MWCNTs with a neutral and hydrophobic tris-hexafluoro acetylacetonate Eu(III) complex, using the nano-extraction methodology.[28] Dismally, the as-prepared hybrid resulted in poor loading and consequently displayed weak emission properties. Hence, with the aim to improve both the filling load and the luminescence of the resulting hybrid material, we decided to exploit the unique CNT–C_{60} interaction to vehiculate LnCs inside CNTs. Inspired by the "nano-carriers" approach as developed by Khlobystov *et al.*[29] who demonstrated the effectiveness of using fullerenes as vehicles for inserting transition metal complexes inside SWCNTs, we also decided to use [60]fullerene derivatives to facilitate and direct the entrance of the LnC within the carbonaceous cavity.

To pursue our goal, we selected the bright tetrakis(2-naphtoyltrifluoro-acetonato) Eu(III) complex ($[\mathbf{EuL_4}]\cdot\mathbf{NEt_4}$)[18a,30] as a guest molecule. This negatively charged compound is known from the literature to efficiently interact with imidazolium-based ionic liquids (ILs)[25,31,32] through both electrostatic and cation–π interactions. Hence, we performed the synthesis of a [60]fullerene derivative bearing an imidazolium appendage ($\mathbf{1\cdot Br}$) capable of ion-pairing with $[\mathbf{EuL_4}]^-$. The resulting ion-paired complex ($\mathbf{1\cdot[EuL_4]}$, Scheme 1) is thus composed of a luminescent "tail" and a [60]fullerene "head", with the latter helping in directing and assisting the encapsulation of the LnC

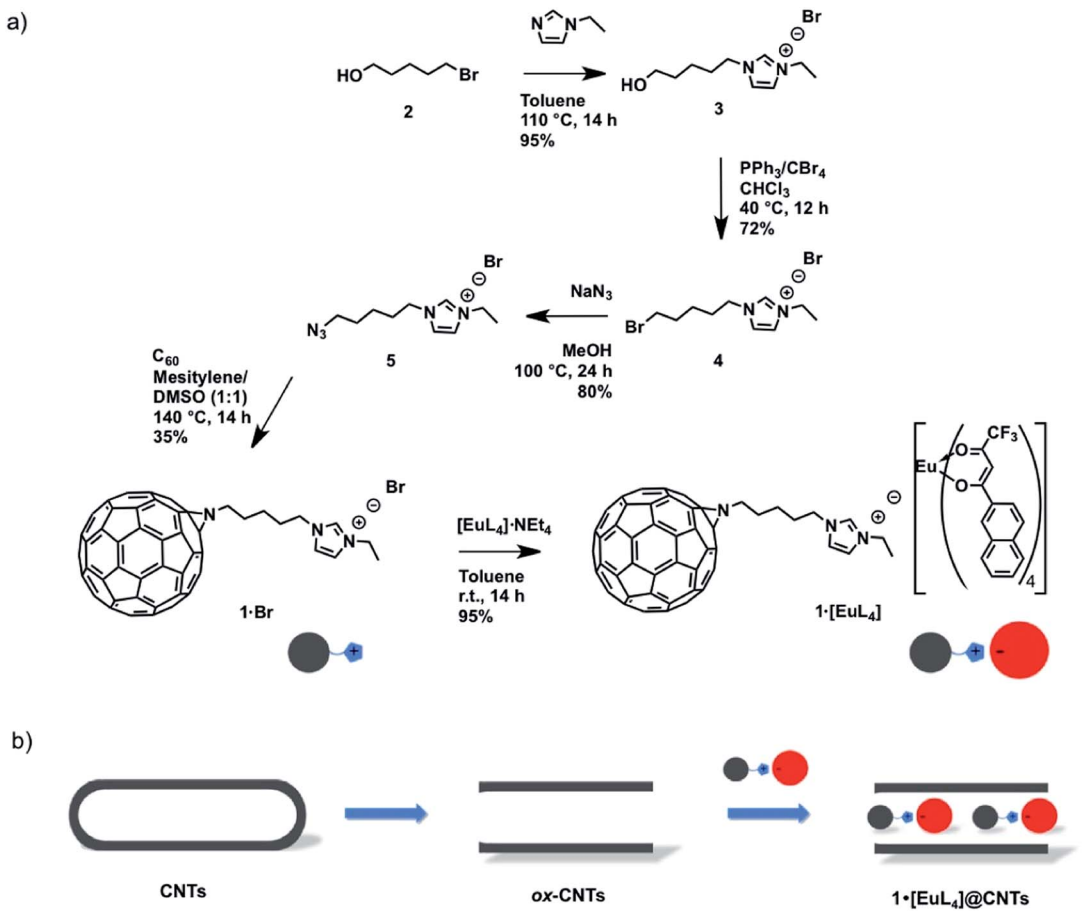

Scheme 1 (a) Synthetic procedures for preparing supramolecular complex $\mathbf{1\cdot[EuL_4]}$. (b) Schematic representation of the filling approach for encapsulating ion-paired complexes.

within the inner cavity of CNTs. Such a design should not only ensure easier encapsulation of the luminescent Eu(III)-complex within the CNTs, but, more interestingly, it should also control the self-organization within the tubular cavity of CNTs with the fullerene moieties of each encapsulated assembly pointing in the same direction, sandwiching different LnCs. To test the difference in encapsulation efficiency as a result of changing the nanotube structure (*e.g.* number of graphitic layers or diameter of the inner channel, to name a few), the [60]fullerene-bearing ion-paired supramolecule was encapsulated, under supercritical CO_2 ($scCO_2$) conditions, inside single-, double- and multi-walled CNTs (SWCNTs, DWCNTs and MWCNTs). Comprehensive characterization was carried out with X-ray photoelectron spectroscopy (XPS) and thermogravimetric analysis (TGA) to determine the elemental and quantitative composition of the hybrids and high-resolution transmission electron microscopy (HRTEM) to unravel the structural morphology. Attenuated total reflectance infrared (ATR-IR) and photoluminescence studies (PL) were used to study the spectroscopic properties of the encapsulated hybrids.

Results and discussion

Synthesis

The [60]fullerene-based cationic nano-carrier (**1·Br**) was synthesized as shown in Scheme 1. C_{60} was subjected to a 1,3-dipolar cycloaddition reaction in the presence of the azido-functionalized imidazolium-based ionic liquid **5**. The latter was synthesized starting from ethyl-imidazolium, which was first alkylated with 5-bromo-pentanol, affording the oxydrilated derivative **3**. Subsequent bromination *via* Appel reaction in the presence of CBr_4 and PPh_3 (**4**), followed by nucleophilic substitution of the terminal Br with the azido functional group provided desired ionic liquid **5** (Scheme 1). Anion exchange metathesis reaction yielding supramolecular complex **1·[EuL$_4$]** was performed by simply stirring a dispersion of the [60] fullerene-appended ionic liquid carrier (**1·Br**) with an excess of precursor ionic complex **[EuL$_4$]·NEt$_4$** (10 equivalents) in toluene for 14 hours in air and at r.t.

Due to their low viscosity, absence of surface tension, and low solvation effect, supercritical fluids (SCFs) provide high diffusivity, approaching that of the gas phase.[33] Among these, $scCO_2$ revealed to be particularly efficient for preparing peapods,[34,35] and for this reason we have decided to employ such an encapsulation protocol.[36] Prior to the encapsulation reaction, CNTs were oxidized[37] to remove their endcaps. Subsequently, the carbonaceous species were annealed in air at 570 °C for 20 minutes to remove any carboxylic groups that could hamper the efficient insertion of the nano-carrier. Encapsulation was finally performed at 50 °C and 150 bar for 96 hours, followed by extensive washing by CH_2Cl_2 to remove any **1·[EuL$_4$]** physisorbed on the external wall of the CNTs (Fig. S1, ESI†).

Qualitative and quantitative characterization of the hybrid material

The elemental composition of the synthesized modified peapods was firstly assessed by XPS analysis. As shown in Table 1 (see also Fig. S2 and 3, ESI†), the oxidized CNTs (ox-SWCNTs, ox-DWCNTs and ox-MWCNTs) only presented the C (1s) and the O (1s) signals at 284 and 533 eV, respectively. The signals relative to **1·[EuL$_4$]**, namely Eu (3d) (1134 eV), F (1s) (686 eV) and N (1s) (401 eV), were detected for **1·[EuL$_4$]@SWCNTs** and **1·[EuL$_4$]@DWCNTs**, whereas hybrid **1·[EuL$_4$]@MWCNTs** exhibited only the signals of N (1s) and F (1s) alongside peculiar signals from the CNTs. The absence of the signal of Eu (3d) is due, not only to a lower amount of encapsulated LnC, but also to the decrease in sensitivity of this analytical technique in the detection of the encapsulated material when increasing the number of graphitic layers of the CNTs (*vide infra*).

TGA analysis of **1·[EuL$_4$]@CNTs** (Fig. 1; see also Fig. S4 and 5, ESI†) confirmed the trend observed *via* XPS analysis. Specifically, in the case of **1·[EuL$_4$]@SWCNTs** and **1·[EuL$_4$]@DWCNTs** the TGA plot revealed two thermal decomposition events. The first event, starting at around 400 °C, is assigned to the decomposition of the encapsulated LnC. The second event, beginning at 550 °C, is the result of the decomposition of the carbon materials: namely the CNT framework and the encapsulated fullerene derivative. This assignment is in agreement with previously reported TGA observations for the encapsulated Eu(III) complex and fullerene peapods, for which the entrapped material resulted characterized by a higher combustion temperature, as compared to the free species because of the shielding effect of the CNT sidewalls.[25,38] Before discussing the extent of the weight loss, it has to be pointed out that both the TGA traces of **1·[EuL$_4$]@SWCNTs** and **1·[EuL$_4$]@DWCNTs** present a slight weight increase below 400 °C, the temperature at which the decomposition of captured **1·[EuL$_4$]** begins (see Fig. S5†). This phenomenon is most probably due to the presence of residual catalyst particles in the CNT samples

Table 1 XPS atomic percentage values obtained for ox-CNTs, and the related encapsulated derivatives[a]

	C[b] [%]	O[b] [%]	N[b] [%]	F[b] [%]	Eu[b] [%]
ox-SWCNTs	96.8 ± 0.6	3.2 ± 0.6	—	—	—
1·[EuL$_4$]@SWCNTs	89.0 ± 0.8	4.4 ± 0.3	0.3 ± 0.1	6.2 ± 0.6	0.1 ± 0.05
ox-DWCNTs	95.6 ± 0.1	4.4 ± 0.1	—	—	—
1·[EuL$_4$]@DWCNTs	91.2 ± 0.2	5.2 ± 0.3	1.3 ± 1.0	2.2 ± 0.4	0.1 ± 0.05
ox-MWCNTs	97.4 ± 0.9	2.6 ± 0.9			
1·[EuL$_4$]@MWCNTs	96.5 ± 0.4	2.0 ± 0.2	1.3 ± 0.2	1.3 ± 0.2	—

[a] Each value is the average of three measurements of the sample. [b] Atomic percentage.

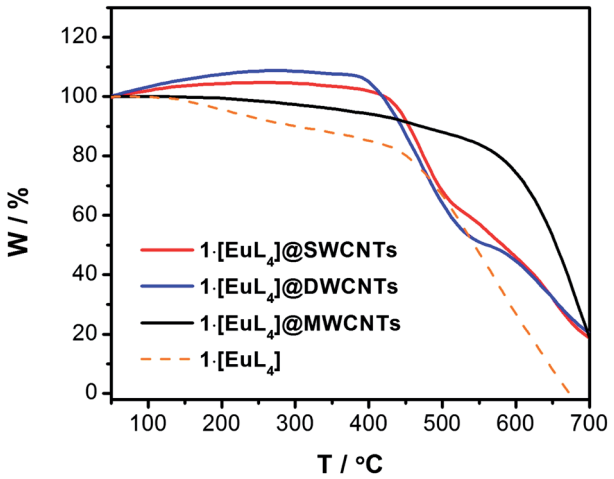

Fig. 1 TGA traces for **1·[EuL$_4$]@SWCNTs** (red line), **1·[EuL$_4$]@DWCNTs** (blue line) and **1·[EuL$_4$]@MWCNTs** (black line). The supramolecular nano-carrier **1·[EuL$_4$]** is also reported for comparison (orange dashed trace). The analysis was recorded in a N_2–air (80 : 20) atmosphere with a heating ramp of 2 °C min^{-1}.

Table 2 TGA analysis data of the **1·[EuL$_4$]@CNTs** hybrids[a]

	TGA [% loss]	Amount[b] [μmol mg^{-1}]
1·[EuL$_4$]@SWCNTs	36.6	0.4
1·[EuL$_4$]@DWCNTs	47.8	0.5
1·[EuL$_4$]@MWCNTs	10.4	0.1

[a] All the experiments were carried out in a N_2–air (80 : 20) atmosphere with a temperature ramp of 2 °C min^{-1}. [b] Calculated considering that all the organic material decomposed was part of complete **[EuL$_4$]$^-$** moieties.

undergoing oxidation when heated in air (Fig. S5†).[39] Contribution to this phenomenon in the case of DWCNTs might also derive from some Eu(III) complex which, on entering the CNTs, might have undergone a transformation into metallic Eu particles (Fig. 2c), species prone to oxidation. However, the extent of the weight loss centered at 450 °C regards exclusively the organic part of the luminescent **[EuL$_4$]$^-$**. Considering this, it was hence possible to assess the amount of LnC encapsulated; 0.4 and 0.5 μmol mg^{-1} for SWCNT and DWCNT hybrids respectively (see Table 2). The TGA profile for pure **1·[EuL$_4$]@MWCNTs** only presented a trivial, yet detectable, weight loss episode.

Morphological characterization

The structure of the resultant endohedral hybrid material was investigated *via* high-resolution transmission electron microscopy (HRTEM). During the analysis, the energy of the electron beam (e^- beam) was lowered to avoid the knock-on damage caused by the collision of electrons from the e^- beam with the atoms of the sample. However, decomposition of **1·[EuL$_4$]** was observed even at 100 kV, often causing just partial visualization of the complex. However, significant amounts of material were observed within the internal cavity of both MWCNTs and DWCNTs (Fig. 2; see also Fig. S6 and 7, ESI†). Specifically, [60] fullerene cages were clearly spotted throughout both samples: in the case of DWCNTs the **1·[EuL$_4$]** units appear well separated, whereas inside MWCNTs the nano-carriers appear tightly agglomerated and clustered. The consistent presence of Eu(III) ions within the DWCNTs, highlighted by the detection of dark spots in the HRTEM images, was also confirmed *via* energy dispersive X-ray (EDX) spectroscopy. Nevertheless, in this sample some Eu metal clusters were also detected, probably formed by complex decomposition followed by the agglomeration of free metal atoms (Fig. 2c).

More interestingly, **1·[EuL$_4$]@SWCNTs** exhibited distinct organization. Indeed, several [60]fullerene cages were observed within the internal cavity of SWCNTs characterized by an internal diameter equal or higher than 2.7 nm (Fig. 3), which corresponds to the minimum diameter required for hosting **1·[EuL$_4$]** (Fig. 3e). In smaller tubes, mainly naked [60]fullerene units were detected. This phenomenon can be explained by taking into account the diameter and the lack of flexibility of the Eu(III) complex. Indeed, **1·[EuL$_4$]** shows a critical diameter of 2.4 nm and is too large to fit within standard SWCNTs (diameter typically around 1.4 nm). In this case, the complex is not able to adjust its conformation in order to squeeze in these tubes, and as it is predicted that the energy gained from the fullerene part of the complex entering the nanotube is significantly higher than the electrostatic interaction holding the "nano-carrier" together, the supramolecular complex will dissociate, with the Eu

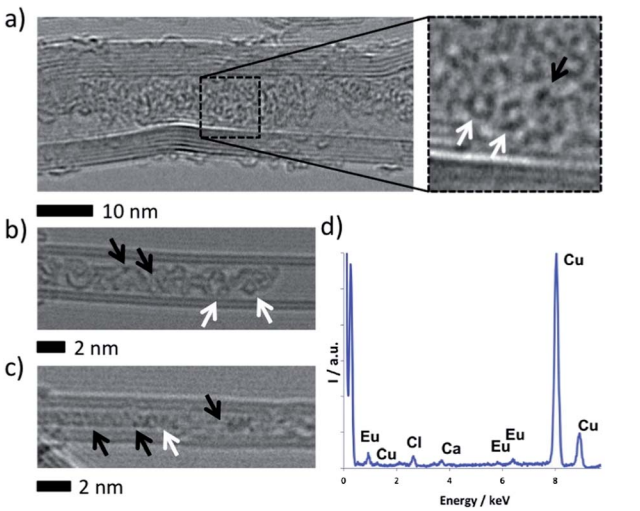

Fig. 2 HRTEM images taken at 100 kV of (a) **1·[EuL$_4$]@MWCNTs** showing large amounts of material within the nanotube channel; the enlarged region shows both fullerene cages (white arrows) and Eu metal atoms (black arrow) which is indicative of successful encapsulation of the Eu complex. (b and c) **1·[EuL$_4$]@DWCNTs** where fullerene cages and significant amounts of Eu metal are observed; the elongated metal cluster present in (c) is a result of e^- beam decomposition of the Eu complex followed by aggregation of the metal atoms to form a rod like structure templated by the shape of the nanotube cavity. (d) The energy dispersive X-ray (EDX) spectrum of the **1·[EuL$_4$]@DWCNTs** confirms the presence of Eu within the nanotubes (Cu peaks are due to the TEM specimen grid and Cl is from the solvent used for sample preparation).

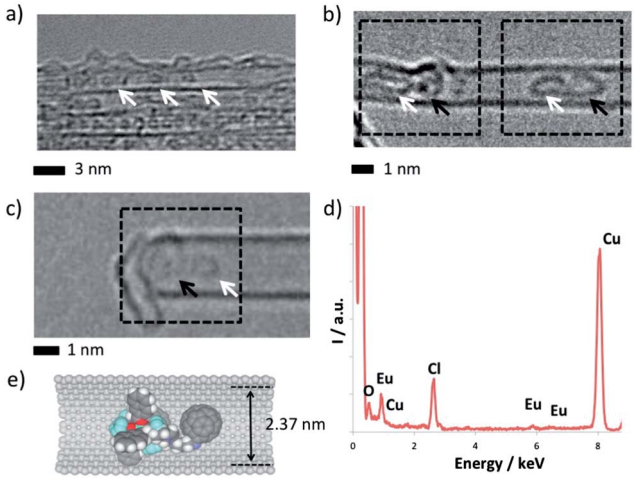

Fig. 3 HRTEM images taken at 100 kV of (a–c) the material obtained from attempts to encapsulate the **1·[EuL$_4$]** in SWCNTs. (a) A significant number of fullerene cages (white arrows) are observed within standard SWCNT channels. (b and c) In wider SWCNTs (d_{NT} = 2.8 nm), the complex is intact and the presence of the fullerene cage (white arrow) and that of the Eu atom (black arrow) is clearly discernable. (d) EDX spectrum of **1·[EuL$_4$]@SWCNTs**. (e) Schematic representation of the complex **1·[EuL$_4$]** within wide SWCNTs.

component stripped off from the fullerene cage (Fig. S8, ESI†). Similar phenomena were previously reported for fullerene metal complexes which are too large to fit within SWCNTs.[40] Nevertheless, several **1·[EuL$_4$]** were found in wider than average SWCNTs (d_{CNT} = 2.7 nm) present in the sample, as clearly evidenced in Fig. 3b and c. The supramolecular nano-carrier **1·[EuL$_4$]** appears as a fullerene cage (white arrow) followed by a dark spot in close proximity, assigned to the single Eu atom. The organic ligands of the Eu(III) complex, being incredibly susceptible to e^- beam damage due to the high number of hydrogen atoms present (immediately stripped out by the e^- beam at 100 kV), appear as an area of grey contrast around the Eu atom. Even though intact, **1·[EuL$_4$]** were unable to enter standard SWCNTs, the amount present in the larger than average tubes behaved as expected. Indeed, when several **1·[EuL$_4$]** couples were observed along the same tube, it was evidenced that the orientation of the single assembly was coherent with that of the others, proving the efficient role of the [60]fullerene moiety as the driving group for the encapsulation. Moreover, a certain degree of regularity in the spacing between the units could be observed, indicating isolation of the luminophores within the structure by the [60]fullerene cages of neighbouring molecules thus preserving their luminescent properties by preventing parasite inter-chromophoric quenching phenomena.

Spectroscopic characterization of the hybrid

While electron microscopy reveals the encapsulated species, it is still important to exclude the presence of adsorbed **1·[EuL$_4$]** on the nanotube surfaces in order to unambiguously assign the spectroscopic features of the encapsulated molecules. Attenuated total reflectance infrared (ATR-IR) spectroscopy was therefore performed to exclude the presence of exohedrally adsorbed material in the hybrid structures (Fig. 4; see also Fig. S9, ESI†).

In fact, it has been previously shown[36] that ATR spectroscopy on CNT hybrids does not detect encapsulated species, but only adsorbed ones. Thus the lack of the ATR signals of **1·[EuL$_4$]**, demonstrates the absence of adsorbed assemblies on the external surface in the purified hybrids. We conclude that the majority of the Eu(III) derivative present in the sample is inside the nanotubes.

Photophysical characterization (PL) of the encapsulated hybrids, **1·[EuL$_4$]@CNTs**, was hence accomplished in the solid state. As displayed in Fig. 5, upon exciting the investigated **1·[EuL$_4$]@CNT** samples at 375 nm (see Fig. S10, ESI†), the typical emission spectrum of the Eu(III) ion, characterized by several emission features between λ = 570 and 700 nm,[36] was

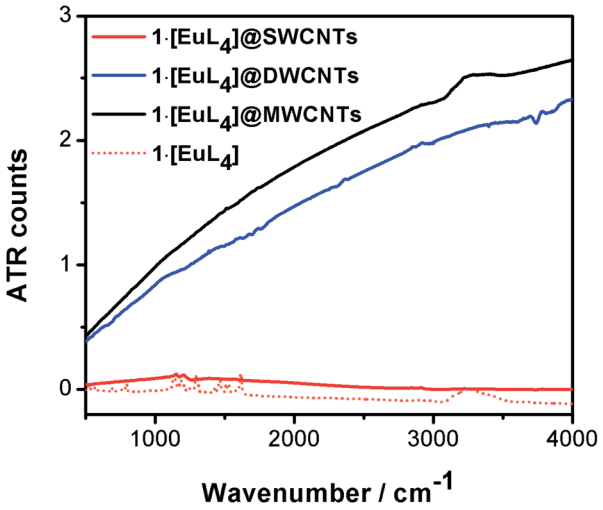

Fig. 4 ATR-IR spectra for **1·[EuL$_4$]** and the nanotube hybrids. No vibrational peaks are discernible in the hybrids, indicating that exohedrally adsorbed species have been completely removed by washing.

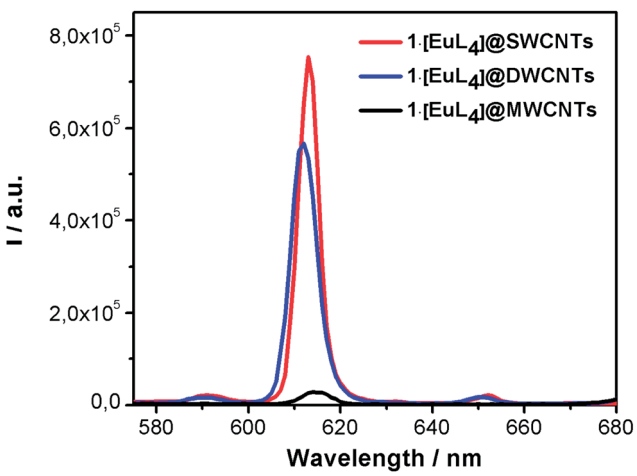

Fig. 5 Emission profiles (λ_{exc} = 375 nm) of KBr pellets (composition ratio: 1 mg of encapsulated material per 10 mg of KBr) containing **1·[EuL$_4$]@SWCNTs** (red trace), **1·[EuL$_4$]@DWCNTs** (blue trace), and **1·[EuL$_4$]@MWCNTs** (black trace).

detected. Specifically, the fingerprint emission of Eu(III) arises from $^5D_0 \rightarrow {}^7F_J$ ($J = 0$–4) f–f electronic transitions. Among others, electric ($^5D_0 \rightarrow {}^7F_2$) and magnetic ($^5D_0 \rightarrow {}^7F_1$) dipolar transitions are predominant in the regions $\lambda = 610$ to 625 and 585 to 600 nm, respectively.

The position of the maximum of the "hypersensitive" electric dipolar transition $^5D_0 \rightarrow {}^7F_2$[41] slightly blue shifts from $\lambda = 614$ nm of **1·[EuL$_4$]** to 613 and 612 nm for **1·[EuL$_4$]@SWCNTs** and **1·[EuL$_4$]@DWCNTs**, and then red-shifts to 615 nm for **1·[EuL$_4$]@MWCNTs**. In contrast, the magnetic dipole transition $^5D_0 \rightarrow {}^7F_1$, largely independent of the ligand field,[42] remained practically unvaried ($\lambda \approx 591$ nm). The intensity ratio between the electric dipole transition and the magnetic dipole transition (R_{21}) affords straightforward indication of the change in the coordination symmetry of the LnC.[43] A value of 36 resulted for both **1·[EuL$_4$]** and **1·[EuL$_4$]@SWCNTs**, whilst it decreased to 34 for **1·[EuL$_4$]@DWCNTs** and to 8 for **1·[EuL$_4$]@MWCNTs**, suggesting that **[EuL$_4$]$^-$** only preserves the symmetry of its free form inside the larger SWCNTs. The absence of distortions supports the occurrence of an ordered encapsulation in which the Eu(III) complexes are mainly isolated and organized within the CNT inner cavity, confirming the HRTEM results. For DWCNTs and MWCNTs, the higher disorder evidenced by HRTEM images reflects a higher distortion of the Eu(III) complex.

The effect of the different packing motifs is further observable following the emission quantum yields and lifetimes. Remarkably the organization of the assemblies can be followed by the photophysical properties of the europium complex. In fact, along the series from SWCNTs to MWCNTs, the hybrids result characterized by increasingly lower emission quantum yields and shorter excited state lifetimes compared to reference **1·[EuL$_4$]** (see Table 3). This trend could be rationalized by considering the organization of the luminescent assemblies imparted by the inner nanotube diameter. Inside large SWCNTs the **1·[EuL$_4$]** assemblies are well-preserved and separated, reducing the emission quenching due to the presence of the fullerene moieties. This was not the case inside DWCNTs and MWCNTs. The more chaotic filling of their internal channel leads to the instauration of indiscriminate interactions between several fullerene cages and a single Eu(III) complex, causing, as already demonstrated in a previous paper,[25] quenching of the emission. Regarding the more complex lifetime patterns observed for **1·[EuL$_4$]@CNTs**, other factors need to be taken into account besides the local ordering. In fact, the possible presence of other emitting Eu-based species inside the CNTs' cavities cannot be excluded to explain the bi-exponential excited state lifetimes of the hybrids. Modification of the structure of **[EuL$_4$]$^-$** might have in fact occurred during the encapsulation process causing either the loss of one or more ligands, yielding **[EuL$_3$]** or **[EuL$_2$]$^+$** species or the formation of clusters (Fig. 2c).

Table 3 Photophysical data for 1·[EuL$_4$]@CNT hybrids

	λ_{em}[a] [nm]	τ[b] [μs]	PLQY[c] (%)
1·[EuL$_4$]	614	256	13
1·[EuL$_4$]@SWCNTs	613	2.40 (20%), 0.17 (80%)	0.02
1·[EuL$_4$]@DWCNTs	612	1.49 (40%), 0.25 (60%)	0.03
1·[EuL$_4$]@MWCNTs	615	0.18 (40%), 0.08 (60%)	0.004[d]

[a] At room temperature, $\lambda_{exc} = 375$ nm. [b] At room temperature, $\lambda_{exc} = 375$ nm, analyzed at 614 nm. [c] Calculated quantum yields according to eqn (1) and (2), ESI†. [d] Estimated quantum yields assuming the same τ_{rad} value as for SWCNTs and DWCNTs.

Conclusions

In conclusion, we have successfully driven the encapsulation of Eu(III) complexes in CNTs by designing and synthesizing a C_{60}-appended ionic liquid nano-carrier. This approach allowed us not only to increase the filling ratio within thinner carbon tubes, namely single and double-walled CNTs, but also to control the organization of the chromophores within the tubular framework. Photophysical investigation showed that the entrapment in different CNTs causes a different degree of emission quenching, particularly affecting the $^5D_0 \rightarrow {}^7F_2$ transition and the luminescence decay time of the hybrids. In the future, appropriate organic functionalization of the external carbon wall, optimization of the filling procedure and the use of different emissive complexes could lead to a brand new class of novel visible-light-emitting CNT-based hybrids. The current work by our group is now devoted to the development of hybrids suitable and compatible for imaging applications in biological systems.[44]

Acknowledgements

DB, LDC and ANK would like to thank the European research council (ERC) for supporting this research. The Namur-Strasbourg collaboration has been supported by the Science Policy Office of the Belgian Federal Government (BELSPO-IAP 7/05 project) and the EU through the FP7-NMP-2012-SMALL-6 "SACS" project (contract no. GA-310651). DB also acknowledges the FRS-FNRS (FRFC contracts no. 2.4.550.09), the "Loterie Nationale", the "TINTIN" ARC project (09/14-023), the MIUR through the FIRB "Futuro in Ricerca" ("SUPRACARBON", contract no. RBFR10DAK6) and the University of Namur (internal funding). MP and OP acknowledge the Polish Ministry of Science & Higher Education (grant no. 938/7. PR UE/2009/7). MEF acknowledges the sectoral operational program for human resources development 2007–2013, co-financed by the European Social Fund (POSDRU 107/1.5/S/76841). MN would like to thank Italian MIUR (FIRB RBAP11C58Y "NanoSolar") for funding. ANK and TC thank the Nottingham Nanotechnology and Nanoscience Centre (NNNC) for access to TEM facilities, and EPSRC for funding. KK acknowledges the Hungarian National Research Fund (OTKA grant no. 105691). The authors thank Dr M. Utczás for expert technical help with the $scCO_2$ filling, and Florent Pineux for technical support for the TGA analysis.

References

1 P. Singh, S. Campidelli, S. Giordani, D. Bonifazi, A. Bianco and M. Prato, *Chem. Soc. Rev.*, 2009, **38**, 2214.

2 (*a*) A. Hashimoto, K. Suenaga, A. Gloter, K. Urita and S. Iijima, *Nature*, 2004, **430**, 870; (*b*) K. Suenaga, H. Wakabayashi, M. Koshino, Y. Sato, K. Urita and S. Iijima, *Nat. Nanotechnol.*, 2007, **2**, 358; (*c*) K. Hirahara, K. Saitoh, J. Yamasaki and N. Tanaka, *Nano Lett.*, 2006, **6**, 1778.

3 C. N. R. Rao, B. C. Satishkumar, A. Govindaraj and M. Nath, *ChemPhysChem*, 2001, **2**, 78.

4 (*a*) A. N. Khlobystov, *ACS Nano*, 2011, **5**, 9306; (*b*) R. Marega and D. Bonifazi, *New J. Chem.*, 2014, **38**, 22–27.

5 D. A. Britz and A. N. Khlobystov, *Chem. Soc. Rev.*, 2006, **35**, 637.

6 H. Ulbricht, G. Moos and T. Hertel, *Phys. Rev. Lett.*, 2003, **90**, 095501.

7 (*a*) S. Berber, Y. K. Kwon and D. Tomanek, *Phys. Rev. Lett.*, 2002, **88**, 185502; (*b*) L. A. Grifalco and M. Hodak, *Phys. Rev. B: Condens. Matter Mater. Phys.*, 2002, **65**, 125404.

8 B. W. Smith, M. Monthioux and D. E. Luzzi, *Nature*, 1998, **396**, 323.

9 J. R. Lakowicz, *Principles of Fluorescence Spectroscopy*, Springer, New York, 2006.

10 M. Shimizu and T. Hiyama, *Chem.–Asian J.*, 2010, **5**, 1516.

11 (*a*) D. Parker and J. A. G. Williams, *J. Chem. Soc., Dalton Trans.*, 1996, 3613; (*b*) J. P. Leonard, C. B. Nolan, F. Stomeo and T. Gunnlaugsson, *Top. Curr. Chem.*, 2007, **281**, 1.

12 K. Yanagi, Y. Miyata and H. Kataura, *Adv. Mater.*, 2006, **18**, 437.

13 (*a*) M. Yudasaka, K. Ajima, K. Suenaga, T. Ichihashi, A. Hashimoto and S. Iijima, *Chem. Phys. Lett.*, 2003, **380**, 42; (*b*) F. Simon, H. Kuzmany, H. Rauf, T. Pichler, J. Bernardi, H. Peterlik, L. Korecz, F. Fulop and A. Janossy, *Chem. Phys. Lett.*, 2004, **383**, 362; (*c*) M. Monthioux, *Carbon*, 2002, **40**, 1809; (*d*) T. Takenobu, T. Takano, M. Shiraishi, Y. Murakami, M. Ata, H. Kataura, Y. Achiba and Y. Iwasa, *Nat. Mater.*, 2003, **2**, 683; (*e*) J. Gao, P. Blondeau, P. Salice, E. Menna, B. Bartova, C. Hebert, J. Leschner, U. Kaiser, M. Milko, C. Ambrosch-Draxl and M. A. Loi, *Small*, 2011, **13**, 1807; (*f*) B. Yan, *RSC Adv.*, 2012, **2**, 9304; (*g*) J. Mohanraj and N. Armaroli, *J. Phys. Chem. Lett.*, 2013, **4**, 767.

14 T. Okazaki, Y. Iizumi, S. Okubo, H. Kataura, Z. Liu, K. Suenaga, Y. Tahara, M. Yudasaka, S. Okada and S. Iijima, *Angew. Chem., Int. Ed.*, 2011, **50**, 4853.

15 (*a*) A. V. Talyzin, I. V. Anoshkin, A. V. Krasheninnikov, R. M. Nieminen, A. G. Nasibulin, H. Jiang and E. I. Kauppinen, *Nano Lett.*, 2011, **11**, 4352; (*b*) M. Fujihara, Y. Miyata, R. Kitaura, O. Nishimura, C. Camacho, S. Irle, Y. Iizumi, T. Okazaki and H. Shinohara, *J. Phys. Chem. C*, 2012, **116**, 15141; (*c*) B. Botka, M. E. Füstös, G. Klupp, D. Kocsis, E. Székely, M. Utczás, B. Simándi, Á. Botos, R. Hackl and K. Kamarás, *Phys. Status Solidi B*, 2012, **249**, 2432; (*d*) B. Botka, M. E. Füstös, H. M. Tóháti, K. Németh, G. Klupp, Zs. Szekrényes, D. Kocsis, M. Utczás, E. Székely, T. Váczi, G. Tarczay, R. Hackl, T. W. Chamberlain, A. N. Khlobystov and K. Kamarás, *Small*, 2013, DOI: 10.1002/smll.201302613.

16 (*a*) K. Binnemans, *Handbook on the Physics and Chemistry of Rare Earths*, Elsevier, Amsterdam, 2005, vol. 35; (*b*) S. Quici, M. Cavazzini, G. Marzanni, G. Accorsi, N. Armaroli, B. Ventura and F. Barigelletti, *Inorg. Chem.*, 2005, **44**, 529; (*c*) S. Quici, G. Marzanni, A. Forni, G. Accorsi and F. Barigelletti, *Inorg. Chem.*, 2004, **43**, 1294; (*d*) L. Armelao, G. Bottaro, S. Quici, M. Cavazzini, M. C. Raffo, F. Barigelletti and G. Accorsi, *Chem. Commun.*, 2007, 2911.

17 T. Pagnot, P. Audebert and G. Tribillon, *Chem. Phys. Lett.*, 2000, **322**, 572.

18 (*a*) K. Binnemans, *Chem. Rev.*, 2009, **109**, 4283; (*b*) J. C. G. Bunzli and S. V. Eliseeva, *J. Rare Earths*, 2010, **28**, 824.

19 (*a*) L. D. Carlos, R. A. S. Ferreira, V. D. Bermudez and S. J. L. Ribeiro, *Adv. Mater.*, 2009, **21**, 509; (*b*) K. Binnemans and C. Görller-Wallrand, *Chem. Rev.*, 2002, **102**, 2303; (*c*) L. Maggini and D. Bonifazi, *Chem. Soc. Rev.*, 2012, **41**, 211.

20 (*a*) G. Accorsi, N. Armaroli, A. Parisini, M. Meneghetti, R. Marega, M. Prato and D. Bonifazi, *Adv. Funct. Mater.*, 2007, **17**, 2975.

21 H.-X. Wu, W.-M. Cao, J. Wang, H. Yang and S.-P. Yang, *Nanotechnology*, 2008, **19**, 345701.

22 (*a*) D. L. Shi, J. Lian, W. Wang, G. K. Liu, P. He, Z. Y. Dong, L. M. Wang and R. C. Ewing, *Adv. Mater.*, 2006, **18**, 189; (*b*) L. Kong, J. Tang, J. Liu, Y. Wang, L. Wang and F. Cong, *Mater. Sci. Eng., C*, 2009, **29**, 85; (*c*) C. Zhao, Y. Song, K. Qu, J. Ren and X. Qu, *Chem. Mater.*, 2010, **22**, 5718; (*d*) X. Xin, M. Pietraszkiewicz, O. Pietraszkiewicz, O. Chernyayeva, T. Kalwarczyk, E. Gorecka, D. Pociecha, H. Li and R. Hoyst, *Carbon*, 2012, **50**, 436; (*e*) V. Divya and M. L. P. Reddy, *J. Mater. Chem. C*, 2013, **1**, 160.

23 D. R. Kauffman, C. M. Shade, H. Uh, S. Petoud and A. Star, *Nat. Chem.*, 2009, **1**, 500.

24 B. Sitharaman, S. Rajamani and K. A. Pramod, *Chem. Commun.*, 2011, **47**, 1607.

25 L. Maggini, H. Traboulsi, K. Yoosaf, J. Mohanraj, J. Wouters, O. Pietraszkiewicz, M. Pietraszkiewicz, N. Armaroli and D. Bonifazi, *Chem. Commun.*, 2011, **47**, 1625.

26 L. Maggini, F. M. Toma, L. Feruglio, J. M. Malicka, T. Da Ros, N. Armaroli, M. Prato and D. Bonifazi, *Chem.–Eur. J.*, 2012, **18**, 5889.

27 L. Maggini, M. Liu, Y. Ishida and D. Bonifazi, *Adv. Mater.*, 2013, **25**, 2462.

28 L. Maggini, J. Mohanraj, H. Traboulsi, A. Parisini, G. Accorsi, N. Armaroli and D. Bonifazi, *Chem.–Eur. J.*, 2011, **17**, 8533.

29 J. Fan, T. W. Chamberlain, Y. Wang, S. Yang, A. J. Blake, M. Schröder and A. N. Khlobystov, *Chem. Commun.*, 2011, **47**, 5696.

30 S. Gago, J. A. Fernandes, J. P. Rainho, R. A. S. Ferreira, M. Pillinger, A. A. Valente, T. M. Santos, L. D. Carlos, P. J. A. Ribeiro-Claro and I. S. Goncalves, *Chem. Mater.*, 2005, **17**, 5077.

31 (*a*) P. Nockemann, E. Beurer, K. Driesen, R. Van Deun, K. Van Hecke, L. Van Meervelt and K. Binnemans, *Chem. Commun.*, 2005, 4354; (*b*) K. Lunstroot, K. Driesen, P. Nockemann, C. Görller-Walrand, K. Binnemans, S. Bellayer, J. Le Bideau and A. Vioux, *Chem. Mater.*, 2006, **18**, 5711.

32 S. M. Bruno, R. A. S. Ferreira, F. A. A. Paz, L. D. Carlos, M. Pillinger, P. Ribeiro-Claro and I. S. Gonçalves, *Inorg. Chem.*, 2009, **48**, 4882.
33 M. Poliakoff and P. J. King, *Nature*, 2001, **412**, 125.
34 A. N. Khlobystov, D. A. Britz, J. Wang, S. A. O'Neil, M. Poliakoff and G. A. D. Briggs, *J. Mater. Chem.*, 2004, **14**, 2852.
35 N. Patel, R. Biswas and M. Maroncelli, *J. Phys. Chem. B*, 2002, **106**, 7096.
36 Á. Botos, A. N. Khlobystov, B. Botka, R. Hackl, E. Székely, B. Simándi and K. Kamarás, *Phys. Status Solidi B*, 2010, **247**, 2743.
37 (*a*) For SWCNTs: D. Bonifazi, C. Nacci, R. Marega, G. Ceballos, S. Modesti, M. Meneghetti and M. Prato, *Nano Lett.*, 2006, **6**, 1408; (*b*) for DWCNTs: R. Marega, G. Accorsi, M. Meneghetti, A. Parisini, M. Prato and D. Bonifazi, *Carbon*, 2009, **47**, 675; (*c*) for MWCNTs: B. Kim and W. M. Sigmund, *Langmuir*, 2004, **20**, 8239.
38 M. Zhang, M. Yudasaka, S. Bandow and S. Iijima, *Chem. Phys. Lett.*, 2003, **369**, 680.
39 (*a*) I. W. Chiang, B. E. Brinson, A. Y. Huang, P. A. Willis, M. J. Bronikowski, J. L. Margrave, R. E. Smalley and R. H. Hauge, *J. Phys. Chem. B*, 2001, **105**, 8297; (*b*) J. Zhao, Y. Su, Z. Yang, L. Wei, Y. Wang and Y. Zhang, *Carbon*, 2013, **58**, 92.
40 T. W. Chamberlain, N. R. Champness, M. Schroder and A. N. Khlobystov, *Chem.–Eur. J.*, 2011, **17**, 668.
41 (*a*) A. Dossing, *Eur. J. Inorg. Chem.*, 2005, 1425; (*b*) A. Beeby, I. M. Clarkson, R. S. Dickins, S. Faulkner, D. Parker, L. Royle, A. S. de Sousa, J. A. G. Williams and M. Woods, *J. Chem. Soc., Perkin Trans. 1*, 1999, 493.
42 J.-C. G. Bunzli, Luminescent Probes, in *Lanthanide Probes in Life, Chemical and Earth Sciences, Theory and Practice*, ed. J.-C. G. Bunzli and G. R. Choppin, Elsevier, New York, 1989, p. 219.
43 J. H. Fosberg, *Coord. Chem. Rev.*, 1973, **10**, 195.
44 (*a*) V. Divya, V. Sankar, K. G. Raghu and M. L. P. Reddy, *Dalton Trans.*, 2013, 15249; (*b*) V. Divya, V. Sankar, K. G. Raghu and M. L. P. Reddy, *Dalton Trans.*, 2013, 12317.

